

**NEARCOM-TVD**  
**A HYBRID TVD SOLVER FOR THE**  
**NEARSHORE COMMUNITY MODEL**  
**DOCUMENTATION AND USER'S MANUAL**

BY  
FENGYAN SHI, JAMES T. KIRBY, TIAN-JIAN (TOM) HSU,  
JIA-LIN CHEN AND RYAN MIERAS

OCTOBER 18, 2013

**RESEARCH REPORT NO. CACR-13-06**



**CENTER FOR APPLIED COASTAL RESEARCH**  
Ocean Engineering Laboratory  
University of Delaware  
Newark, Delaware 19716

## **Acknowledgements**

This model development was sponsored by the Office of Naval Research, Coastal Geosciences Program through grant N00014-10-1-0406, the Delaware Sea Grant, NA10OAR4170084 and the Bureau of Ocean Energy Management (BOEM) grant M10PC00118.

## **Abstract**

The report documents a new version of the Nearshore Community Model (NearCoM) initially developed during the National Oceanography Partnership Program (NOPP). The model couples a wave model SWAN, a nearshore circulation model SHORECIRC and a sediment model in a fully parallelized computational environment. The wave module SWAN is modified based on the structured grid Version 40.51AB, which is the last stable version before the release of the unstructured grid version UnSWAN. The circulation module SHORECIRC is improved numerically using a hybrid TVD solver. The sediment module uses two optional sediment transport formulas. One is Soulsby's formula (Soulsby, 1997) which takes into account total load sediment transport by both waves and currents. The other option for sediment transport is Kobayashi et al's (2007) formula which was initially used in the CSHORE one-dimensional model and was modified for two-dimensional applications. This development emphasizes numerical improvements, including 1) a conservative form of SHORECIRC equations in non-orthogonal curvilinear coordinates; 2) MUSCL-TVD solver with adaptive Runge-Kutta time stepping; 3) wetting-drying moving boundary condition with incorporation of HLL construction method into the scheme; 4) fully parallel computation with equal CPU load for each processor. The documentation provides derivations of the conservative form of theoretical equations in generalized curvilinear coordinates, re-arrangement of pressure gradient term in order to obtain a numerically well-balanced form, detailed numerical schemes, users' manual and examples.

# Contents

<b>1</b>	<b>Introduction</b>	<b>6</b>
<b>2</b>	<b>Theory</b>	<b>7</b>
2.1	SHORECIRC equations . . . . .	7
2.2	SWAN equations . . . . .	11
2.3	Soulsby's sediment transport formula . . . . .	12
2.4	Kobayashi's sediment transport formula . . . . .	12
2.5	Seabed evolution equation . . . . .	14
<b>3</b>	<b>Numerical schemes for SHORECIRC</b>	<b>14</b>
3.1	Compact form of governing equations . . . . .	14
3.2	Spatial discretization . . . . .	15
3.3	Time stepping . . . . .	17
3.4	Wetting-drying schemes for shallow water . . . . .	17
3.5	Boundary conditions . . . . .	17
<b>4</b>	<b>SWAN-SHORECIRC coupling and parallelization</b>	<b>18</b>
<b>5</b>	<b>Users' Manual</b>	<b>21</b>
5.1	Program outline and flow chart . . . . .	21
5.2	Permanent variables associated with coupling . . . . .	21
5.3	Installation and compilation . . . . .	23
5.4	Input . . . . .	24
5.5	Output . . . . .	32
<b>6</b>	<b>Examples</b>	<b>32</b>
6.1	An idealized case . . . . .	32
6.2	Simulation of longshore currents . . . . .	38
<b>7</b>	<b>Appendix A: Extended form of tensor expression</b>	<b>41</b>
<b>8</b>	<b>References</b>	<b>42</b>

## List of Figures

1	Definition of an angle between $x$ -axis and beach-normal direction. . . . .	13
2	Variation in model performance with number of processors for a 1800 x 1800 domain. Straight line indicates arithmetic speedup. Actual performance is shown in the curved line. . . . .	19
3	An example of domain decomposition in SWAN and SHORECIRC/SEDIMENT. . . . .	20
4	Flow chart of the main program. . . . .	22
5	Idealized bathymetry. . . . .	33
6	(Top panel) wave height (color) and currents. (Bottom panel) surface elevation (color) and currents. . . . .	34
7	For the giving wave condition of wave height=1m, wave incident angle = 10 degree (a) Comparison of longshore current velocity profiles computed by NearCoM-TVD (blue) and Longuet-Higgins (1970b) (red). The breaker line location of Longuet-Higgins formula is given as $XB=-250$ m (b) Wave height distribution computed by NearCoM-TVD (SWAN). . . . .	38
8	Idealized bathymetry. . . . .	39
9	(Top panel) wave height (Bottom panel) current velocity . . . . .	40

# 1 Introduction

The Nearshore Community Model System, NearCoM, was developed during the National Oceanography Partnership Program (NOPP), for predicting waves, currents, sediment transport and bathymetric change in the nearshore ocean. The modeling system consists of a suite of ‘modules,’ each of which handles a focused subset of the physical processes being studied. A master program (Shi et al., 2005) is used to link those modules (usually integration of three modules: wave, circulation and seabed) and to handle data input, output and internal data transfer between modules. The NearCoM system provides various wave, circulation and sediment modules based on different theories and numerical methods, which can be configured and extended by users themselves. A frequently used example of NearCoM is a combination of a wave module REF/DIF-1 (Kirby and Dalrymple, 1992), circulation module SHORECIRC (Svendsen, et al., 2003) and sediment module HH (Haas and Hanes, 2004). An application of coupling a wave module and a 3-D circulation module (POM) has been reported recently by Newberger and Allen (2007).

Because NearCoM focuses on predicting nearshore waves and wave-induced nearshore processes, modules in the original NearCoM system were developed specifically for nearshore applications, basically between the shoreline and about 10 m water depth. There are difficulties that limit the general application of NearCoM to some ocean-exposed coastal regions. For example, in tidal inlet regions, the tidal forcing is not considered in the model because of unknown tidal boundary conditions; wave input is somewhat arbitrary as there is no link to a large scale wave generation and transformation model which could predict spatial inhomogeneities in incident wave conditions; and sediment transport processes may also need boundary conditions associated with offshore sediment sources or river discharges. Most recently, Shi et al. (2011) integrated the wave model SWAN and a modified version of SHORECIRC in the system to extend its application to a large scale, beach inlet system.

In the aspect of numerics, there have been several improvements in numerical approaches for SHORECIRC since it was released. The original version of SHORECIRC was based on SHORECIRC equations in Cartesian coordinates and implemented using finite difference schemes in which time stepping was treated by the predictor-corrector scheme, while spatial differencing was handled by a second-order central differencing scheme. A curvilinear version of SHORECIRC was developed based on a coordinate transformation from Cartesian to a generalized curvilinear grid system (Shi et al., 2003). The curvilinear SHORECIRC was further enhanced using a CFL-free numerical scheme in order to improve computational efficiency (Shi et al., 2007).

There is a growing demand recently to use NearCoM in various coastal applications, such as wave-current interaction in an inlet system, storm-induced coastal inundation, beach and dune erosions, tidal flat processes, and etc. Some large-scale processes such as tides, wind and wind-wave generation play important roles in those applications. Those applications raise concerns about model efficiency and stability in a long-time simulation. Although the recent version with a CFL-free numerical scheme is efficient in terms of a large time step, there is an ‘ADI effect’ caused by an extreme large Courant number (Casulli and Cheng, 1992). The computational codes for all versions of SHORECIRC are based on serial computation using a single computer processor.

In this work, we developed a new code of SHORECIRC using a hybrid method combining the finite-volume and finite-difference — TVD-type scheme (Toro, 2009). This scheme has been proved to be stable and robust in modeling wave breaking and moving shorelines in the most recent development of the fully-nonlinear Boussinesq model with a TVD solver (FUNWAVE-TVD, Shi et al., 2011a, 2011b, Tehranirad et al., 2011, Kirby et al., 2011). Good performance of the TVD scheme was also found in several Boussinesq and shallow water equation models developed by other recent authors (Tonelli and Petti, 2009, Roeber et al., 2010, Shiach and Mingham, 2009, Erduran et al., 2005, and others).

A conservative form of SHORECIRC equations was derived in order to use the hybrid numerical scheme. The surface elevation gradient term was rearranged following Shi et al. (2011) to obtain a numerically well-balanced form. In contrast to previous temporal schemes, which usually require uniform time-stepping, we used adaptive time stepping based on the Runge-Kutta method. In the hybrid spatial scheme, a MUSCL reconstruction technique, which is accurate up to the fourth-order, was used in the Riemann solver.

The wave model SWAN, the circulation model SHORECIRC and the sediment module are integrated as a single model in the same parallelized model framework. The domain decomposition technique, with the Message Passing Interface (MPI), is used for the SHORECIRC code in connection with the decomposed SWAN grid through global mapping. The parallel scheme has a feature of equal CPU load for each processor, which is more efficient in contrast to the recent model coupling framework of WRF, SWAN and ROMS by Warner et al. (2008) which use the Model Coupling Toolkid (MCT) to distribute CPUs unevenly for each processor.

This report provides derivations of the conservation form of theoretical equations with a well-balanced pressure gradient term, numerical schemes, and users' manual. The last part of this report uses an idealized case to demonstrate basic model setup for a general application and illustrates some model applications to problems of wave-induced nearshore circulation.

## 2 Theory

### 2.1 SHORECIRC equations

SHORECIRC is a quasi-3D nearshore circulation model for prediction of wave-induced nearshore circulation. It is a 2D horizontal model which incorporates the effect of the vertical structure of horizontal flows. In Putrevu and Svendsen (1999), the instantaneous horizontal velocity is split as

$$u_{ins}^\alpha = u'^\alpha + u_w^\alpha + u^\alpha + u_1^\alpha \quad (1)$$

wherer  $u'^\alpha$ ,  $u_w^\alpha$ ,  $u^\alpha$  and  $u_1^\alpha$  are, respectively, the turbulence component, the wave component, the component of depth-averaged and short-wave-averaged velocity, and the vertical variation of the short-wave-averaged velocity. In generalized curvilinear coordinates,  $()^\alpha$  represents the contravariant component of a vector. We use superscription for contravariant component and subscription for Cartesian component (hereafter). Note that the depth-averaged and short-wave-averaged velocity

$u^\alpha$  is defined by the ‘Lagrangian’ averaging as

$$u^\alpha = \frac{1}{h} \int_h^{\zeta} \overline{u_{ins}^\alpha} dz \quad (2)$$

where  $\zeta$  represents the instantaneous surface elevation. This split is different from Haas et al. (2003) who used the ‘Eulerian’ concept for their split. For the Lagrangian averaging method, it is assumed that

$$\int_{-h}^{\eta} u_1^\alpha dz = -Q_w^\alpha \quad (3)$$

where  $Q_w^\alpha$  or  $Q_{w\alpha}$  (Cartesian expression) is short wave flux,  $\eta$  is wave-averaged surface elevation. The SHORECIRC equations can be written in contravariant form as

$$\frac{\partial \eta}{\partial t} + \frac{1}{J} \frac{\partial}{\partial x_\alpha} [J u^\alpha H] = 0 \quad (4)$$

$$\frac{\partial u^\alpha H}{\partial t} + (u^\alpha u^\beta H)_{,\beta} + f^\alpha + \frac{1}{\rho} (S^{\alpha\beta})_{,\beta} + g H g^{\alpha\beta} \frac{\partial \eta}{\partial x_\beta} + \frac{\tau_b^\alpha}{\rho} - \frac{\tau_s^\alpha}{\rho} - (H \tau^{\alpha\beta})_{,\beta} + \text{ROT} = 0 \quad (5)$$

where  $H = h + \eta$ , in which  $h$  is still water depth,  $\rho$  is water density,  $f^\alpha$  represents the Coriolis force,  $(\ )_{,\alpha}$  represents the covariant derivative, and  $g^{\alpha\beta}$  is the contravariant metric tensor.  $S^{\alpha\beta}$  is radiation stress defined by Longuet-Higgins and Stewart (1962, 1964). Its contravariant form can be found in Shi et al. (2003).  $\tau_s^\alpha$  and  $\tau_b^\alpha$  are wind stress and bottom stress, respectively.  $\tau^{\alpha\beta}$  represents turbulent shear stress which is assumed depth-uniform:

$$\tau^{\alpha\beta} = \nu_t T^{\alpha\beta} \quad (6)$$

where  $T^{\alpha\beta}$  is the rate of strain tensor,  $\nu_t$  is the eddy viscosity coefficient. The eddy viscosity accounts for both wave-breaking and bottom generated turbulence and is evaluated by

$$\nu_t = C_1 \kappa \sqrt{\frac{f_{cw}}{2}} u_0 h + M h \left(\frac{D}{\rho}\right)^{1/3} + \nu_{t0} + \nu_s \quad (7)$$

where  $\kappa$  is the von Karman constant ( $k \sim 0.4$ ),  $u_0$  is the short-wave particle velocity amplitude from a wave model,  $D$  is the energy dissipation per unit area from a wave model.  $C_1 \sim 0.2$  and  $M = 0.08$  as in Svendsen et al. (2003). The constant  $\nu_{t0}$  is an empirical measure of the background eddy viscosity. A large value (10-20 times turbulent viscosity) can be used if the 3D dispersion is switched off in order to get a comparable result with 3D dispersion switched on.

Wind stress in SHORECIRC was computed using Van Dorn’s (1953) formula:

$$\tau_s^\alpha = f_a \rho_a |\mathbf{W}| W_\alpha \quad (8)$$

where  $\mathbf{W}$  is wind speed at a 10 m elevation above the water surface,  $f_a$  is the drag coefficient which can be found in Dean and Dalrymple (1991),  $\rho_a$  represents air density. For the bottom

stress in SHORECIRC, we adopted the formulation for wave-averaged bottom stress for combined currents and waves given by Svendsen and Putrevu (1990) which is written as

$$\tau_b^\alpha = f_{cw}\rho u_0(\beta_1 u_b^\alpha + \beta_2 u_w^\alpha). \quad (9)$$

where  $u_w$  is the amplitude of short-wave particle velocity evaluated at the bottom using wave bulk parameters,  $f_{cw}$  is the friction factor,  $u_b^\alpha$  is the current velocity at the bottom obtained from the theoretical solution of the equation for the vertical variation,  $\beta_1$  and  $\beta_2$  are the weight factors for the current and wave motion given by Svendsen and Putrevu (1990) and evaluated using linear wave theory.

ROT in equation (5) represents rest of terms associated with atmospheric pressure and 3D dispersion (see details in Shi et al., 2003).

The equations above are in the contravariant form which is not suitable for the combined finite-volume and finite-difference numerical scheme. The conservative form of the equations can be obtained using expressions which combine Cartesian and contravariant components (Shi and Sun, 1995, Shi et al., 1998). The coordinate transformation is performed between the Cartesian coordinates  $x_\alpha$  and generalized curvilinear coordinates  $\xi^\alpha$ .

The contravariant components of velocity vector can be expressed by

$$u^\alpha = u_\beta L_\beta^\alpha \quad (10)$$

where  $u_\beta$  is the Cartesian component of velocity vector and

$$L_\beta^\alpha = \frac{\partial \xi^\alpha}{\partial x_\beta} \quad (11)$$

A derivative in the Cartesian coordinates can be replaced with that in the curvilinear coordinates using

$$\frac{\partial}{\partial x_\alpha} = L_\alpha^\beta \frac{\partial}{\partial \xi^\beta} \quad (12)$$

A conservative form of SHORECIRC equations can be written as

$$\frac{\partial \eta}{\partial t} + \frac{1}{J} \frac{\partial JP^\alpha}{\partial \xi^\alpha} = 0 \quad (13)$$

$$\begin{aligned} \frac{\partial H u_\alpha}{\partial t} + \frac{1}{J} \frac{\partial}{\partial \xi^\beta} \left[ JP^\beta u_\alpha + \frac{1}{2} g(\eta^2 + 2\eta h) JL_\alpha^\beta \right] + f_\alpha - g\eta \frac{1}{J} \frac{\partial}{\partial \xi^\beta} (h JL_\alpha^\beta) \\ + \frac{1}{\rho} \frac{1}{J} \frac{\partial}{\partial \xi^\gamma} (S_{\alpha\beta} JL_\beta^\gamma) + \frac{1}{J} \frac{\partial}{\partial \xi^\gamma} (\tau_{\alpha\beta} JHL_\beta^\gamma) + \frac{\tau_\alpha^b}{\rho} - \frac{\tau_\alpha^s}{\rho} + \text{ROT} = 0 \end{aligned} \quad (14)$$

where  $P^\alpha = H u^\alpha$ , denoting the contravariant component of volume flux,  $f_\alpha$  represents the Cartesian component of the Coriolis term, i.e.,  $(-fHv, fHu)$  in which  $(u, v)$  represent the velocity in

Cartesian coordinates,  $S_{\alpha\gamma}$  represents the Cartesian component of radiation stress,  $\tau_\alpha^b$  and  $\tau_\alpha^s$  are the Cartesian components of bottom stress and wind stress. Note that the metric identity (Thompson et al., 1985) law is used for derivation of (14), i.e.,

$$\frac{\partial}{\partial \xi^\alpha}(JL_\beta^\alpha) \equiv 0 \quad (15)$$

The surface gradient term is treated following Shi et al. (2011) who reorganized this term in order to make it well-balanced in a MUSCL-TVD scheme for a general order. The expression in curvilinear coordinates can be written as

$$-gHJ \frac{\partial \eta}{\partial x_\alpha} = -\frac{\partial}{\partial \xi^\alpha} \left[ \frac{1}{2} g(\eta^2 + 2\eta h) JL_\beta^\alpha \right] + g\eta \frac{\partial}{\partial \xi^\alpha} (hJL_\beta^\alpha) \quad (16)$$

There are several advantages in using equations (13) and (14) versus (4) and (5). First, they are a conservative form which can be implemented using a hybrid numerical scheme. Second, all forcing terms reduce to vector form in Cartesian coordinates in contrast to the contravariant form in (5). Third, the radiation stress term  $S_{\alpha\beta}$  uses the original form defined in Cartesian coordinates, thus there is no need to make a transformation for the second-order tensor. The disadvantage is that (14) contains both the Cartesian component  $u_\alpha$  and the contravariant component  $P^\alpha$ . However, in terms of the hybrid numerical scheme used in the study, it is convenient to solve both of the variables using the explicit numerical scheme, rather than the implicit numerical scheme used for (5) in Shi et al., (2007).

The treatment of turbulent shear stress terms follows the scheme for the radiation stress terms. The extended form of the shear stress terms can be found in Appendix A.  $\tau_{\alpha\beta}$  is defined in the Cartesian coordinates as

$$\tau_{\alpha\beta} = \nu_t \left( \frac{\partial u_\alpha}{\partial x_\beta} + \frac{\partial u_\beta}{\partial x_\alpha} \right) \quad (17)$$

The derivatives in the Cartesian coordinates are calculated using (12).

The equation governing the vertical structure of horizontal velocity can be solved analytically using the lowest order of the equation for vertical variation of current:

$$\frac{\partial u_{1\alpha}}{\partial t} - \frac{\partial}{\partial z} \left( \nu_t \frac{\partial u_{1\alpha}}{\partial z} \right) = F_\alpha \quad (18)$$

where  $\nu_t$  is the eddy viscosity coefficient; and  $F_\alpha$  is a general form of the local forcing described as

$$F_\alpha = \frac{1}{\rho h} f_{w\alpha} - f_\alpha^{lrad} + \frac{\tau_\alpha^b}{\rho h} - \frac{\tau_\alpha^s}{\rho h} \quad (19)$$

where  $f_\alpha^{lrad}$  represents the local radiation stress defined by Putrevu and Svendsen (1999). In the offshore domain without wave forcing, (19) reduces to

$$F_\alpha = \frac{\tau_\alpha^b}{\rho h} - \frac{\tau_\alpha^s}{\rho h} \quad (20)$$

The solution of equation (18) can be obtained analytically following Putrevu and Svendsen (1999). The bottom current velocity  $u_\alpha^b$  can be evaluated using  $u^\alpha$  and  $u_{1\alpha}$  at bottom:

$$u_\alpha^b = u_\alpha + u_{1\alpha}(z = -h) \quad (21)$$

## 2.2 SWAN equations

In this section, we briefly summarize equations used in SWAN. Detailed documentation is referred to SWAN Users' Manual at <http://swanmodel.sourceforge.net/>.

The spectral wave model SWAN (Booij et al., 1999, Ris et al., 1999) solves the wave action balance equation. In generalized curvilinear coordinates, the governing equation reads

$$\frac{\partial N}{\partial t} + \frac{1}{J} \frac{\partial(JC_g^\alpha)}{\partial \xi_\alpha} + \frac{\partial(C_{g\sigma}N)}{\partial \sigma} + \frac{\partial(C_{g\theta}N)}{\partial \theta} = \frac{S}{\sigma} \quad (22)$$

where  $\xi_\alpha$  represents curvilinear coordinates defined the same as in the curvilinear SHORECIRC equations,  $\sigma$  is the relative angular frequency,  $\theta$  is propagation direction of each wave component,  $C_g^\alpha$  represents the contravariant component of the energy propagation speed which can be obtained using coordinate transformation

$$C_g^\alpha = C_{g\beta}L_\beta^\alpha \quad (23)$$

in which  $C_{g\beta} = (C_{gx}, C_{gy})$  in the rectangular Cartesian coordinates. Equation (22) is written in a tensor-invariant form in order to make it consistent with the circulation equations. The extended numerical form can be found in Booij et al. (1997).  $C_{g\sigma}$  and  $C_{g\theta}$  denote energy propagation speeds in the  $\sigma$  and  $\theta$ -spaces, respectively.  $S$  represents source and sink terms in terms of energy density representing the effects of wave generation, dissipation and nonlinear wave-wave interactions.  $N$  is wave action defined by

$$N = E(\xi^\alpha, \sigma, \theta, t)/\sigma \quad (24)$$

in which  $E$  is wave energy density.

Current effects on wave transformation are presented by the following calculations:

1) Total group velocity including the current component

$$C_{g\alpha} = \frac{1}{2} \left( 1 + \frac{2kd}{\sinh 2kd} \right) \frac{\sigma k_\alpha}{|\mathbf{k}|^2} + u_{E\alpha} \quad (25)$$

where  $k_\alpha$ , or  $\mathbf{k}$ , represents the wave number,  $d$  is short-wave-averaged water depth, and  $d = h + \eta$ .  $u_{E\alpha} = u_\alpha - Q_{w\alpha}/H$  in terms of undertow or Eulerian mean velocity.

2) Changes to relative frequency

$$C_\sigma = \frac{\partial \sigma}{\partial d} \left( \frac{\partial d}{\partial t} + \mathbf{u}_E \cdot \nabla d \right) - C_g \mathbf{k} \cdot \frac{\partial \mathbf{u}_E}{\partial s} \quad (26)$$

3) Wave refraction by current included in

$$C_\theta = -\frac{1}{k} \left( \frac{\partial \sigma}{\partial d} \frac{\partial d}{\partial m} + \mathbf{k} \cdot \frac{\partial \mathbf{u}_E}{\partial m} \right) \quad (27)$$

where  $s$  is the space coordinate in direction  $\theta$  and  $m$  is a coordinate normal to  $s$ .

### 2.3 Soulsby's sediment transport formula

The total load transport by waves plus currents derived by Soulsby's (1997) can be written as

$$q_\alpha = A_s z u_\alpha \left[ \left( u_\alpha^2 + \frac{0.018}{C_d} u_{rms}^2 \right)^{1/2} - u_\alpha^{cr} \right]^{2.4} (1 - 1.6 \tan \beta) \quad (28)$$

where

$$A_{sb} = \frac{0.005h(d_{50}/d)^{1.2}}{[(s-1)gd_{50}]^{1.2}} \quad (29)$$

$$A_{ss} = \frac{0.012d_{50}D_*^{-0.6}}{[(s-1)gd_{50}]^{1.2}} \quad (30)$$

$$A_s = A_{sb} + A_{ss} \quad (31)$$

$u_{rms}$  is root-mean-square wave orbital velocity,  $C_d$  is drag coefficient due to current alone,  $u_\alpha^{cr}$  represents threshold current velocity given by Van Rijn (1984),  $\beta$  is the slope of bed in streamwise direction,  $s$  is the specific gravity, and

$$D_* = \left[ \frac{g(s-1)}{\nu} \right]^{1/3} d_{50} \quad (32)$$

### 2.4 Kobayashi's sediment transport formula

Kobayashi et al. (2007) recently proposed sediment transport formulas for the cross-shore and longshore transport rates of suspended sand and bedload on beaches based on laboratory experiments and field data. For suspended sand, the suspended sediment volume,  $V_s$ , per unit horizontal bottom area was introduced as

$$V_s = P_s \frac{e_B D_r + e_f D_f}{\rho g (s-1) w_f} (1 + S_b^2)^{0.5} \quad (33)$$

where  $S_b$  is cross-shore bottom slope;  $e_B$  and  $e_f$  are suspension efficiencies for energy dissipation rates  $D_r$  and  $D_f$  due to wave breaking and bottom friction, respectively;  $w_f$  is the sediment fall velocity;  $P_s$  is the probability of sediment suspension formulated in Kobayashi et al. (2007). The corresponding cross-shore and alongshore suspended sediment transport rates may be expressed as

$$q_{sc} = a \bar{U}_c V_s; \quad q_{sl} = \bar{V}_l V_s \quad (34)$$

where  $a$  is an empirical suspended load parameter;  $\bar{U}_c$  is the Eulerian-mean cross-shore current which consists of wave-induced return flow (undertow) and tidal current in the cross-shore direction;  $\bar{V}_c$  is alongshore current which includes wave-induced alongshore current and tidal current in the alongshore direction. Subscriptions  $c$  and  $l$  represent cross-shore and longshore, respectively (hereafter).

In Kobayashi et al., the vector  $(\bar{U}_c, \bar{V}_l)$  is defined specifically in cross-shore/alongshore directions which may not be appropriate for general 2-D applications, especially for complex coastal geometry. Here, we define  $\vec{V} = (\bar{U}, \bar{V})$  as the Eulerian-mean current vector in general Cartesian coordinates which is not restricted to the cross-shore/alongshore orientation. Thus formula (34) can be written in a general form using coordinate rotation as

$$q_{sx} = (a\bar{U} \cos^2 \alpha + a\bar{V} \sin \alpha \cos \alpha + \bar{U} \sin^2 \alpha - \bar{V} \sin \alpha \cos \alpha)V_s \quad (35)$$

$$q_{sy} = (a\bar{V} \sin^2 \alpha + a\bar{U} \sin \alpha \cos \alpha + \bar{V} \cos^2 \alpha - \bar{U} \sin \alpha \cos \alpha)V_s \quad (36)$$

in which  $\alpha$  is the angle between the  $x$ -axis and beach-normal direction as shown in Figure 1.

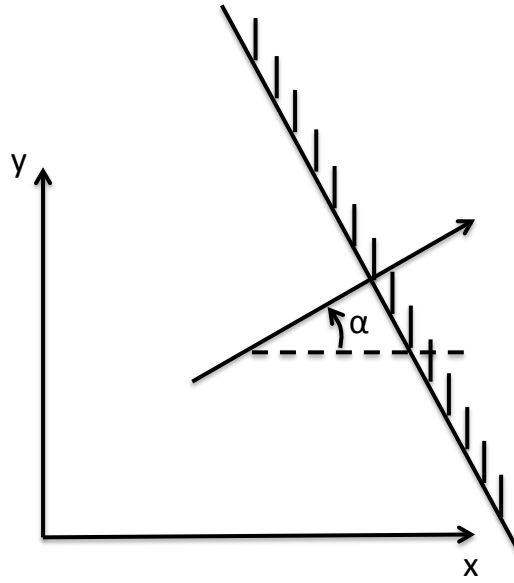


Figure 1: Definition of an angle between  $x$ -axis and beach-normal direction.

The bedload transport rates can be expressed as

$$q_{bc} = \frac{bP_b}{g(s-1)} \sigma_T^3 (1 + U_* V_*^2 + 2F_m \sin \theta) G_s \quad (37)$$

$$q_{bl} = \frac{bP_b}{g(s-1)}\sigma_T^3 [V_*(1 + U_*^2 + V_*^2) - 2r_m \sin \theta] \quad (38)$$

where  $b$  is an empirical bedload parameter,  $\sigma_T$  is the standard deviation of the oscillatory depth-averaged velocity with zero mean,  $(U_*, V_*) = (\bar{U}_c/\sigma_T, \bar{V}_l/\sigma_T)$ ,  $\theta$  is the wave angle, and

$$r_m = -(U_* \cos \theta + V_* \sin \theta) \quad (39)$$

$$F_m = V_* \cos \theta - U_* \sin \theta \quad (40)$$

$G_s$  is the bottom slope function expressed by

$$\begin{cases} G_s = \tan \phi / (\tan \phi + S_b) & \text{for } -\tan \phi < S_b < 0 \\ G_s = (\tan \phi - 2S_b) / (\tan \phi - S_b) & \text{for } 0 < S_b < \tan \phi \end{cases} \quad (41)$$

in which  $\phi$  is the angle of internal friction of the sediment and  $\tan \phi \simeq 0.63$  for sand.

In a general Cartesian system,  $(q_{bc}, q_{bl})$  are converted to  $(q_{bx}, q_{by})$  using

$$q_{bx} = q_{bc} \cos \alpha - q_{bl} \sin \alpha, \quad q_{by} = q_{bc} \sin \alpha + q_{bl} \cos \alpha \quad (42)$$

## 2.5 Seabed evolution equation

The sea bed evolution equation can be described using sediment transport flux in generalized curvilinear coordinates:

$$(1-p) \frac{\partial h}{\partial t} + \frac{1}{J} \frac{\partial J f_{mor} q_{\beta} L_{\beta}^{\alpha}}{\partial \xi^{\alpha}} = 0 \quad (43)$$

where  $p$  is the bed porosity,  $f_{mor}$  represents a morphology factor. Equation (43) is solved using the same TVD scheme as in SHORECIRC.

## 3 Numerical schemes for SHORECIRC

### 3.1 Compact form of governing equations

The compact form of the governing equations can be written as

$$\frac{\partial \Psi}{\partial t} + \nabla \cdot \Theta(\Psi) = \mathbf{S} \quad (44)$$

where  $\Psi$  and  $\Theta(\Psi)$  are the vector of conserved variables and the flux vector function, respectively, and are given by

$$\Psi = \begin{pmatrix} J\eta \\ JP \\ JQ \end{pmatrix} \quad (45)$$

$$\Theta = \begin{pmatrix} JP\mathbf{i} + JQ\mathbf{j} \\ \left[ JPu + \frac{1}{2}g(\eta^2 + 2\eta h)JL_1^1 \right] \mathbf{i} + \left[ JQu + \frac{1}{2}g(\eta^2 + 2\eta h)JL_1^2 \right] \mathbf{j} \\ \left[ J Pv + \frac{1}{2}g(\eta^2 + 2\eta h)JL_2^1 \right] \mathbf{i} + \left[ JQv + \frac{1}{2}g(\eta^2 + 2\eta h)JL_2^2 \right] \mathbf{j} \end{pmatrix}. \quad (46)$$

$$\mathbf{S} = \begin{pmatrix} 0 \\ \frac{1}{\rho} (F_{\text{Wx}} - \tau_x^b + \tau_x^s - f_x, -ROT_x) \\ \frac{1}{\rho} (F_{\text{Wy}} - \tau_y^b + \tau_y^s - f_y - ROT_y) \end{pmatrix}, \quad (47)$$

where  $(u, v)$  represent Cartesian components of velocity,  $(P, Q) = (Hu^1, Hu^2)$ , the contravariant components of flow flux,  $(\tau_x^b, \tau_y^b)$ ,  $(\tau_x^s, \tau_y^s)$ ,  $(f_x, f_y)$  and  $(ROT_x, ROT_y)$  represent the bottom friction, wind stress, Coriolis forcing and the rest of terms in  $x$  and  $y$  directions, respectively.  $(F_{\text{Wx}}, F_{\text{Wy}})$  are the gradient of radiation stresses expressed by

$$F_{\text{Wx}} = - \left[ \frac{\partial}{\partial \xi^1} (S_{xx}JL_1^1 + S_{xy}JL_2^1) + \left[ \frac{\partial}{\partial \xi^2} (S_{xx}JL_1^2 + S_{xy}JL_2^2) \right] \right] \quad (48)$$

$$F_{\text{Wy}} = - \left[ \frac{\partial}{\partial \xi^1} (S_{xy}JL_1^1 + S_{yy}JL_2^1) + \left[ \frac{\partial}{\partial \xi^2} (S_{xy}JL_1^2 + S_{yy}JL_2^2) \right] \right] \quad (49)$$

The reason to put the wave forcing as a source term rather than a flux term is that the forcing is calculated directly from SWAN in a curvilinear grid.

### 3.2 Spatial discretization

A combined finite-volume and finite-difference method was applied to the spatial discretization. For the flux terms and the first-order derivative terms, MUSCL-TVD schemes from the 2nd-order to 4th-order are implemented in the present model. The multi-order MUSCL-TVD scheme can be written in a compact form according to Erduran et al. (2005) who modified Yamamoto et al.'s (1995) fourth-order approach. In the  $x$ -direction, for example, the combined form of the interface construction can be written as follows:

$$\phi_{i+1/2}^L = \phi_i + \frac{1}{4} \left[ (1 - \kappa_1)\chi(r)\Delta^*\phi_{i-1/2} + (1 + \kappa_2)\chi(1/r)\Delta^*\phi_{i+1/2} \right] \quad (50)$$

$$\phi_{i-1/2}^R = \phi_i - \frac{1}{4} \left[ (1 + \kappa_1)\chi(r)\Delta^*\phi_{i-1/2} + (1 - \kappa_2)\chi(1/r)\Delta^*\phi_{i+1/2} \right] \quad (51)$$

where  $\phi_{i+1/2}^L$  is the constructed value at the left-hand side of the interface  $i + \frac{1}{2}$  and  $\phi_{i-1/2}^R$  is the value at the right-hand side of the interface  $i - \frac{1}{2}$ . The values of  $\Delta^*\phi$  are evaluated as follows:

$$\begin{aligned} \Delta^*\phi_{i+1/2} &= \Delta\phi_{i+1/2} - \kappa_2\Delta^3\bar{\phi}_{i+1/2}/6, \\ \Delta\phi_{i+1/2} &= \phi_{i+1} - \phi_i, \\ \Delta^3\bar{\phi}_{i+1/2} &= \Delta\bar{\phi}_{i+3/2} - 2\Delta\bar{\phi}_{i+1/2} + \Delta\bar{\phi}_{i-1/2}, \end{aligned}$$

$$\begin{aligned}
\Delta\bar{\phi}_{i-1/2} &= \text{minmod}(\Delta\phi_{i-1/2}, \Delta\phi_{i+1/2}, \Delta\phi_{i+3/2}), \\
\Delta\bar{\phi}_{i+1/2} &= \text{minmod}(\Delta\phi_{i+1/2}, \Delta\phi_{i+3/2}, \Delta\phi_{i-1/2}), \\
\Delta\bar{\phi}_{i+3/2} &= \text{minmod}(\Delta\phi_{i+3/2}, \Delta\phi_{i-1/2}, \Delta\phi_{i+1/2})
\end{aligned} \tag{52}$$

In (52), minmod represents the minmod limiter and is given by

$$\text{minmod}(j, k, l) = \text{sign}(j) \max\{0, \min[|j|, 2\text{sign}(j)k, 2\text{sign}(j)l]\}. \tag{53}$$

$\kappa_1$  and  $\kappa_2$  in (50) and (51) are control parameters for orders of the scheme in the compact form. The complete form with  $(\kappa_1, \kappa_2) = (1/3, 1)$  is the fourth-order scheme given by Yamamoto et al. (1995).  $(\kappa_1, \kappa_2) = (1/3, 0)$  yields a third-order scheme, while the second-order scheme can be retrieved using  $(\kappa_1, \kappa_2) = (-1, 0)$ .

$\chi(r)$  in (50) and (51) is the limiter function. The original scheme introduced by Yamamoto et al. (1998) uses the Minmod limiter as used in (52). Erduran et al. (2005) found that the use of the van-Leer limiter for the third-order scheme gives more accurate results. Their finding was confirmed by using the present model in the benchmark tests for wave runup conducted by Tehranirad et al. (2011). The van-Leer limiter can be expressed as

$$\chi(r) = \frac{r + |r|}{1 + r} \tag{54}$$

where

$$r = \frac{\Delta^*\phi_{i+1/2}}{\Delta^*\phi_{i-1/2}}. \tag{55}$$

The numerical fluxes are computed using a HLL approximate Riemann solver

$$\Theta(\Psi^L, \Psi^R) = \begin{cases} \Theta(\Psi^L) & \text{if } s_L \geq 0 \\ \Theta^*(\Psi^L, \Psi^R) & \text{if } s_L < 0 < s_R \\ \Theta(\Psi^R) & \text{if } s_R \leq 0, \end{cases} \tag{56}$$

where

$$\Theta^*(\Psi^L, \Psi^R) = \frac{s_R\Theta(\Psi^L) - s_L\Theta(\Psi^R) + s_Ls_R(\Psi^R - \Psi^L)}{s_R - s_L} \tag{57}$$

The wave speeds of the Riemann solver are given by

$$s_L = \min(\mathbf{V}^L \cdot \mathbf{n} - \sqrt{g(h + \eta)^L}, u_s - \sqrt{\varphi_s}), \tag{58}$$

$$s_R = \max(\mathbf{V}^R \cdot \mathbf{n} + \sqrt{g(h + \eta)^R}, u_s + \sqrt{\varphi_s}), \tag{59}$$

in which  $u_s$  and  $\varphi_s$  are estimated as

$$u_s = \frac{1}{2}(\mathbf{V}^L + \mathbf{V}^R) \cdot \mathbf{n} + \sqrt{g(\eta + h)^L} - \sqrt{g(\eta + h)^R} \tag{60}$$

$$\sqrt{\varphi_s} = \frac{\sqrt{g(\eta+h)^L} + \sqrt{g(\eta+h)^R}}{2} + \frac{(\mathbf{V}^L - \mathbf{V}^R) \cdot \mathbf{n}}{4} \quad (61)$$

and  $\mathbf{n}$  is the normalized side vector for a cell face.

### 3.3 Time stepping

The third-order Strong Stability-Preserving (SSP) Runge-Kutta scheme for nonlinear spatial discretization (Gottlieb et al., 2001) was adopted for time stepping. The scheme is given by

$$\begin{aligned} \Psi^{(1)} &= \Psi^n + \Delta t(-\nabla \cdot \Theta(\Psi^n) + \mathbf{S}^{(1)}) \\ \Psi^{(2)} &= \frac{3}{4}\Psi^n + \frac{1}{4} \left[ \Psi^{(1)} + \Delta t \left( -\nabla \cdot \Theta(\Psi^{(1)}) + \mathbf{S}^{(2)} \right) \right] \\ \Psi^{n+1} &= \frac{1}{3}\Psi^n + \frac{2}{3} \left[ \Psi^{(2)} + \Delta t \left( -\nabla \cdot \Theta(\Psi^{(2)}) + \mathbf{S}^{n+1} \right) \right] \end{aligned} \quad (62)$$

in which  $\Psi^n$  denotes  $\Psi$  at time level  $n$ .  $\Psi^{(1)}$  and  $\Psi^{(2)}$  are values at intermediate stages in the Runge-Kutta integration.

An adaptive time step is chosen, following the Courant-Friedrichs-Lewy (CFL) criterion:

$$\Delta t = C \min \left( \min \frac{\Delta x}{|u_{i,j}| + \sqrt{g(h_{i,j} + \eta_{i,j})}}, \min \frac{\Delta y}{|v_{i,j}| + \sqrt{g(h_{i,j} + \eta_{i,j})}} \right) \quad (63)$$

where  $C$  is the Courant number and  $C = 0.5$  was used in the following examples.

### 3.4 Wetting-drying schemes for shallow water

The wetting-drying scheme for modeling a moving boundary is straightforward. The normal flux  $\mathbf{n} \cdot \mathbf{M}$  at the cell interface of a dry cell is set to zero. A mirror boundary condition is applied to the high-order MUSCL-TVD scheme. It may be noted that the wave speeds of the Riemann solver (58) and (59) for a dry cell are modified as

$$s_L = \mathbf{V}^L \cdot \mathbf{n} - \sqrt{g(h+\eta)^L}, \quad s_R = \mathbf{V}^L \cdot \mathbf{n} + 2\sqrt{g(h+\eta)^L} \quad (\text{right dry cell}) \quad (64)$$

and

$$s_L = \mathbf{V}^R \cdot \mathbf{n} - \sqrt{g(h+\eta)^R}, \quad s_R = \mathbf{V}^R \cdot \mathbf{n} + 2\sqrt{g(h+\eta)^R} \quad (\text{left dry cell}) \quad (65)$$

### 3.5 Boundary conditions

To incorporate tide and river inflow into the circulation module, two types of open boundary conditions are implemented. One is the surface clamped boundary condition that reads at tidal open boundaries

$$\eta = \eta_0 \quad \text{at tidal open boundaries} \quad (66)$$

where  $\eta_0$  is measured or predicted surface elevations at open boundaries. The other is the specified flux boundary condition that is usually used at river boundaries:

$$P^\alpha = Q_\beta^{\text{flux}} L_\beta^\alpha \quad (67)$$

where  $Q_\beta^{\text{flux}}$  is the specified volume flux per unit width.

## 4 SWAN-SHORECIRC coupling and parallelization

For the SHORECIRC code, we used a domain decomposition technique to subdivide the problem into multiple regions and assign each subdomain to a separate processor core. Each subdomain region contains an overlapping area of ghost cells, three-row deep, as required by the highest-order (the fourth order) MUSCL-TVD scheme in the model. The Message Passing Interface (MPI) with non-blocking communication is used to exchange data in the overlapping region between neighboring processors.

To investigate performance of the parallel program, numerical simulations of an idealized case are tested with different numbers of processors on a Linux cluster located at University of Delaware. The test case is set up in a numerical grid of  $1800 \times 1800$  cells. Figure 2 shows the model speedup versus number of processors. It can be seen that performance scales nearly proportional to the number of processors, with some delay caused by inefficiencies in parallelization, such as inter-processor communication time.

For the SWAN code, we used the existing domain decomposition scheme which is slightly different from the SHORECIRC code. The version 40.51AB of SWAN uses a single-direction domain decomposition and takes into account the number of dry points in the grid splitting. Because of the different domain decompositions between SHORECIRC and SWAN, it is difficult to directly pass variables between the decomposed domains. We now use a two-step mapping method which first gathers a passing variable into the global domain and then distributes it into each sub-domain. Dry points in SWAN are set to be wet with a small water depth (1 mm) in order to make an equal split of a computational domain.

Figure 3 shows an example of domain decomposition in SWAN and SHORECIRC.

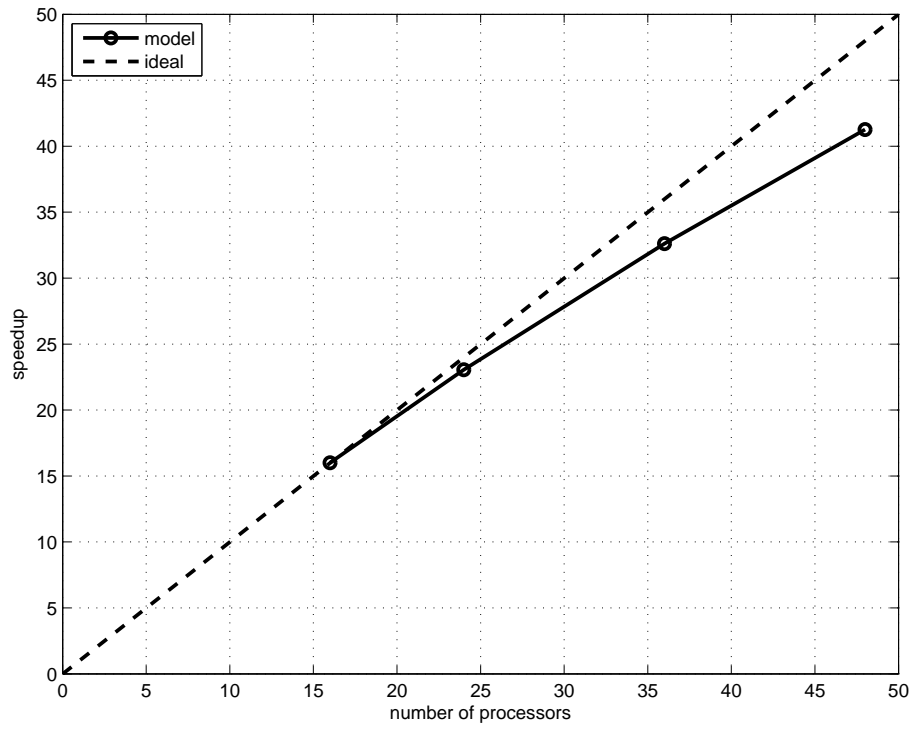


Figure 2: Variation in model performance with number of processors for a 1800 x 1800 domain. Straight line indicates arithmetic speedup. Actual performance is shown in the curved line.

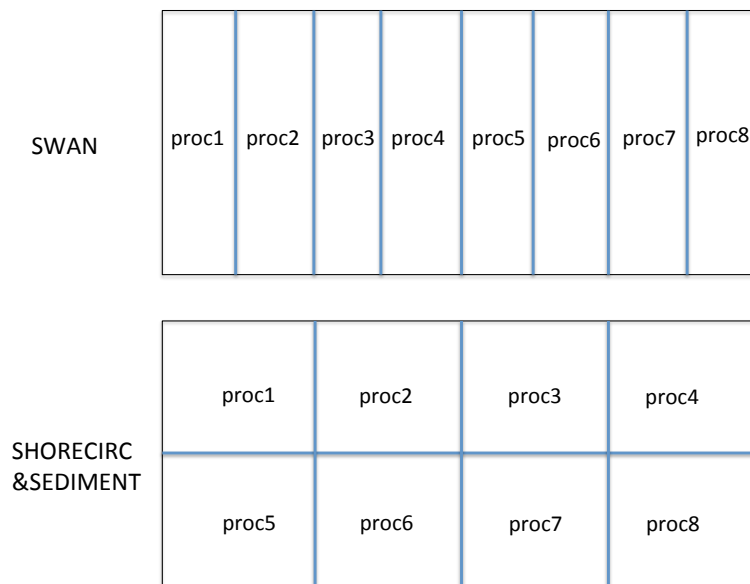


Figure 3: An example of domain decomposition in SWAN and SHORECIRC/SEDIMENT.

## 5 Users' Manual

### 5.1 Program outline and flow chart

The code was written using Fortran 90 with the `c` preprocessor (`cpp`) statements for separation of the source code. Arrays are dynamically allocated at runtime. Precision is selected using the `selected_real_kind` Fortran intrinsic function defined in the makefile. The default precision is single.

The present version of NearCoM-TVD includes a number of options including (1) choice of serial or parallel code (2) Cartesian or curvilinear coordinate, (3) samples.

The flow chart is shown in Figure 4.

### 5.2 Permanent variables associated with coupling

Depth(): still water depth  $h$  at element point

DepthX(): still water depth  $h$  at x-interface

DepthY(): still water depth  $h$  at y-interface

Eta(): surface elevation, for dry point,  $\text{Eta}() = \text{MinDepth} - \text{Depth}()$ , `MinDepth` is specified in `input.txt`.

Eta0():  $\eta$  at previous time level

MASK(): 1 - wet, 0 - dry

MASK\_STRUC(): 0 - permanent dry point

U(): depth-averaged  $u$

V(): depth-averaged  $v$

Uc(): contravariant component of depth-averaged velocity in  $\xi_1$  direction

Vc(): contravariant component of depth-averaged velocity in  $\xi_2$  direction

HU():  $(h + \eta)u$  at element

HV():  $(h + \eta)v$  at element

P():  $(h + \eta)U$  at x-interface for Cartesian, and  $(h + \eta)Uc$  at  $\xi_1$ -interface curvilinear

Q():  $(h + \eta)V$  at y-interface for Cartesian, and  $(h + \eta)Vc$  at  $\xi_2$ -interface curvilinear

Fx(): numerical flux  $F$  at x-interface

Fy(): numerical flux  $F$  at y-interface

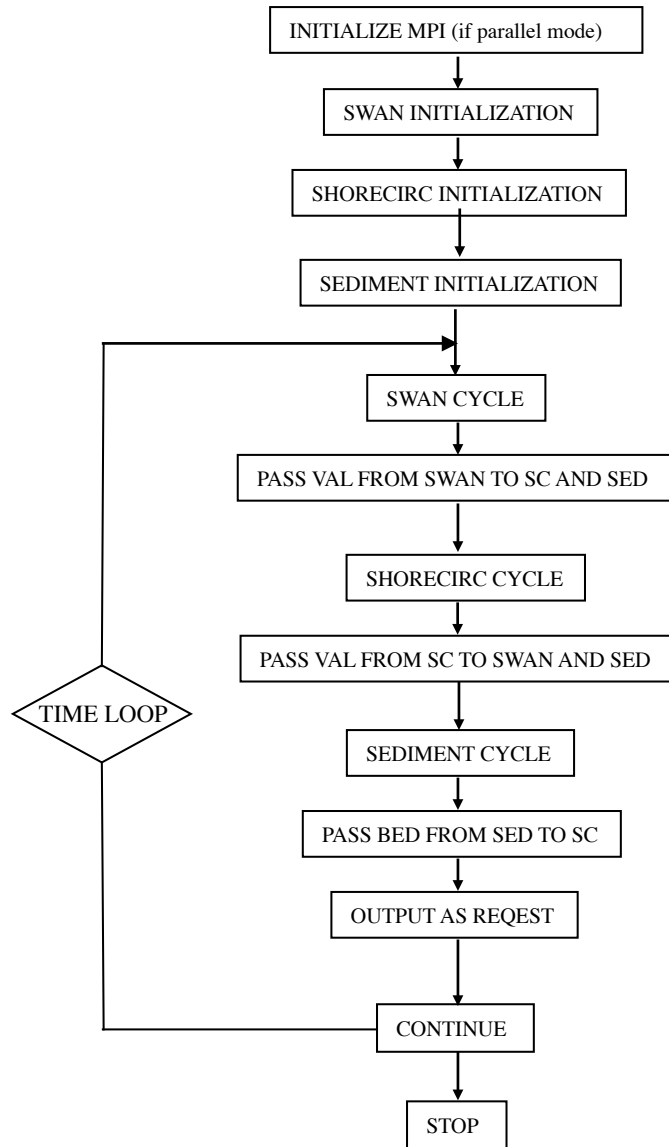


Figure 4: Flow chart of the main program.

Gx(): numerical flux G at x-interface  
 Gy(): numerical flux G at y-interface  
 Ubar():  $HU$  for Cartesian and  $JHU$  for curvilinear  
 Vbar():  $HV$  for Cartesian and  $JHV$  for curvilinear  
 EtaRxL():  $\eta$  Left value at x-interface  
 EtaRxR():  $\eta$  Right value at x-interface  
 EtaRyL():  $\eta$  Left value at y-interface  
 EtaRyR():  $\eta$  Right value at y-interface  
 HxL(): total depth Left value at x-interface  
 HxR(): total depth Right value at x-interface  
 HyL(): total depth Left value at y-interface  
 HyR(): total depth Right value at y-interface  
 HUXL():  $(h + \eta)u$  Left value at x-interface  
 HUXR():  $(h + \eta)u$  Right value at x-interface  
 HVyL():  $(h + \eta)v$  Left value at y-interface  
 HVyR():  $(h + \eta)v$  Right value at y-interface  
 PL(): Left P value at x-interface  
 PR(): Right P value at x-interface  
 QL(): Left Q value at y-interface  
 QR(): Right Q value at y-interface

### 5.3 Installation and compilation

NearCoM-TVD is distributed in a compressed file. To install the programs, first, uncompress the package. Then use

```
> tar xvf *.tar
```

to extract files from the uncompressed package. The extracted files will be distributed in two new directories: /CIRC\_SWAN and /work.

To compile the program, go to /CIRC\_SWAN and modify Makefile if needed. There are several necessary flags in Makefile needed to specify below.

-DDOUBLE\_PRECISION: use double precision, default is single precision.  
-DPARALLEL: use parallel mode, default is serial mode.  
-DSAMPLES: include all samples, default is no sample included.  
-DCURVILINEAR: curvilinear version, otherwise Cartesian.  
    **NOTE:** setting curvilinear is a must for SWAN and SHORECIRC coupled model.  
-DSEDIMENT: include sediment and seabed modules.  
-DINTEL: INTEL compiler.  
-DRESIDUAL: include tidal residual calculation.  
-DSTATIONARY: stationary mode for SHORECIRC  
CPP: path to CPP directory.  
FC: Fortran compiler.

Then execute

```
> make clean  
> make
```

The executable file 'nearcom' will be generated and copied from /CIRC\_SWAN to /work/. Note: use 'make clean' after any modification of Makefile.

To run the model, go to /work. Modify INPUT if needed and run.

## 5.4 Input

Following are descriptions of parameters in input.txt (**NOTE:** all parameter names are case sensitive).

**SWAN INPUT:** refer to SWAN manual. Model run time is set in SWAN model. For example,

```
COMPUTE NONSTAT 20081114.160000 1 MI 20081114.230000
```

The above setting means model run start from 2008 11 14 16:00 to 2008 11 14 23:00. The model calls swan at  $DT_{swan} = 1$  minute. The loop number for SHORECIRC and SEDIMENT is estimated by  $DT_{swan}$  and the time step of SHORECIRC (time varying).

### **IMPORTANT SETTINGS IN SWAN:**

- 1) in SET, always set CARTESIAN in order to make a grid orientation consistent with SHORECIRC
- 2) in SET, always set [inrhog] as 1 to get a true wave energy dissipation.
- 3) in COMPUTE, always set NONSTAT mode.

## **WAVE CURRENT INTERACTION**

SWAN\_RUN: logical parameter to run SWAN

SHORECIRC\_RUN: logical parameter to run SHORECIRC

WC\_BOUND\_WEST: west bound region (number of grid points) in which wave-current is inactive.

WC\_BOUND\_EAST : east bound region (number of grid points) in which wave-current is inactive.

WC\_BOUND\_SOUTH : south bound region (number of grid points) in which wave-current is inactive.

WC\_BOUND\_NORTH: north bound region (number of grid points) in which wave-current is inactive.

WC\_LAG : time delay for wave-current interaction

TITLE: title for SHORECIRC log file

## **SPECIFICATION OF MULTI-PROCESSORS**

PX: processor numbers in X

PY : processor numbers in Y

**NOTE:** PX and PY must be consistent with the number of processors defined in mpirun command, e.g., mpirun -np n (where  $n = px \times py$ ).

## **SPECIFICATION OF WATER DEPTH**

DEPTH\_TYPE: depth input type.

DEPTH\_TYPE=DATA: from a depth file.

The program includes several simple bathymetry configurations such as

DEPTH\_TYPE=FLAT: flat bottom, need DEPTH\_FLAT

DEPTH\_TYPE=SLOPE: plane beach along  $x$  direction. It needs three parameters: slope,SLP, slope starting point, Xslp and flat part of depth, DEPTH\_FLAT

DEPTH\_FILE: bathymetry file if DEPTH\_TYPE=DATA, file dimension should be Mglob x Nglob with the first point as the south-west corner. The read format in the code is shown below.

```
DO J=1,Nglob
```

```
READ(1,*)(Depth(I,J),I=1,Mglob)
```

```
ENDDO
```

DEPTH\_FLAT: water depth of flat bottom if DEPTH\_TYPE=FLAT or DEPTH\_TYPE=SLOPE (flat part of a plane beach).

SLP: slope if DEPTH\_TYPE=SLOPE

Xslp: starting  $x$  (m) of a slope, if DEPTH\_TYPE=SLOPE

### **SPECIFICATION OF RESULT FOLDER**

RESULT\_FOLDER: result folder name, e.g., RESULT\_FOLDER = /Users/fengyanshi/tmp/

### **SPECIFICATION OF DIMENSION**

Mglob: global dimension in  $x$  direction.

Nglob: global dimension in  $y$  direction.

**NOTE:** For parallel runs, Mglob and Nglob can be divided by PX and PY, respectively. MAX(Mglob,Nglob) can be divided by  $PX \times PY$ .

### **SPECIFICATION OF STATIONARY MODE**

N\_ITERATION: the iteration number for stationary mode of SHORECIRC (set -DSTATIONARY in Makefile).

WATER\_LEVEL\_FILE: the file name of water level file containing time and water level, for stationary mode. The following example shows the format.

```
water levels for stationary mode
5 - number of water level data
0.0 0.0 ! Time (s), Level (m)
3600.0 0.5
7200.0 0.8660
10800.0 1.0
14400.0 0.866
18000.0 0.5
```

### **SPECIFICATION OF TIME**

PLOT\_INTV: output interval in seconds (Note, output time is not exact because adaptive dt is used.)

SCREEN\_INTV: time interval (s) of screen print.

PLOT\_INTV\_STATION: time interval (s) of gauge output

### **SPECIFICATION OF GRID**

DX: grid size(m) in  $x$  direction, for Cartesian mode

DY: grid size(m) in  $y$  direction, for Cartesian mode

X\_FILE: name of file to store  $x$  for curvilinear mode

Y\_FILE: name of file to store  $y$  for curvilinear mode

**NOTE:** data format is the same as the depth data shown above.

CORI.CONSTANT: logical parameter for constant Coriolis parameter

LATITUDE: latitude if constant Coriolis parameter is used

LATITUDE\_FILE: name of file to store latitude at every grid point if not constant Coriolis

**NOTE:** data format is the same as the depth data shown above.

### BOUNDARY CONDITIONS

ETA.CLAMPED: logical parameter for surface elevation clamped condition

V.CLAMPED: logical parameter for velocity clamped condition

FLUX.CLAMPED: logical parameter for flux clamped condition

TIDE\_FILE: name of file to store tidal constituents

**DATA FORMAT:** please refer to mk\_tide.f90. The formula of surface elevation at a tidal boundary can be expressed by

$$\eta_0(t) = \sum_{n=1}^N a_0(\mathbf{x}, n) f_c(n) \cos \left( \frac{2\pi}{T(n)} t - \phi(\mathbf{x}, n) + (V_0 + u_0)(n) \right) \quad (68)$$

where  $a_0$  and  $\phi$  represent amplitude and phase lag, respectively, for a harmonic constituent at location  $\mathbf{x}$ .  $T$  is tidal period.  $f_c$  and  $(V_0 + u_0)$  are the lunar node factor and the equilibrium argument, respectively, for a constituent.

The following is an example of M2 + O1.

tidal boundary conditions

150 — number of days from Jan 1, to simulation date

2 — number of constituents

1.000 0.000 —  $f_c$  and  $(V_0 + u_0)$  for M2

0.980 0.000 —  $f_c$  and  $(V_0 + u_0)$  for O1

80 — number of tidal boundary points

1 , 1 — (i,j) grid location of tidal boundary

12.420 1.200 21.000 —  $T$ , amplitude  $a_0$  and phase lag  $\phi$  for M2

24.000 0.3 30.100 –  $T$ , amplitude  $a_0$  and phase lag  $\phi$  for O1  
 2 , 1 — (i,j) grid location of tidal boundary  
 12.420 1.200 21.000 —  $T$ , amplitude  $a_0$  and phase lag  $\phi$  for M2  
 24.000 0.3 30.100 –  $T$ , amplitude  $a_0$  and phase lag  $\phi$  for O1  
 3 , 1  
 ...

FLUX\_FILE: name of file to store time series of flux (e.g., unit width river flux)

**DATA FORMAT:**

title  
 Number of data, Number of flux points  
 I, J, River orientation  
 Time, Flux, Angle in Cartesian  
 ...

where (I,J) represent grid points of river location. River orientation represents the direction from which a river flows in the IMAGE domain (for curvilinear coordinates). Use W,E,S and N for the orientation. For example, ‘W’ represents a river flowing into the domain from the west boundary (in IMAGE domain for curvilinear coordinates).

Please refer to mk\_river.f90. The following is an example.

```
river flux boundary condition
5 2 ! NumTimeData, NumFluxPoint
1 38 W ! I, J, River_Orientation
0.000 0.200 0.000
360000.000 0.200 0.000
720000.000 0.200 0.000
1080000.000 0.200 0.000
1440000.000 0.200 0.000
1 39 W ! I, J, River_Orientation
0.000 0.200 0.000
360000.000 0.200 0.000
720000.000 0.200 0.000
1080000.000 0.200 0.000
1440000.000 0.200 0.000
end of file
```

**WIND CONDITION**

Spatially uniform wind field is assumed in this version.

WindForce: logical parameter for wind condition, T or F.

WIND\_FILE: name of file for a time series of wind speed.

**DATA FORMAT:** the following is an example of wind data.

wind data

100 - number of data

0.0 , -10.0 0.0 — time(s),  $w_u$ ,  $w_v$  (m/s)

2000.0, -10.0, 0.0

8000.0, -10.0, 0.0

...

Cdw: wind stress coefficient for the quadratic formula.

### **SPECIFICATION OF INITIAL CONDITION**

INT\_UVZ : logical parameter for initial condition, default is FALSE

ETA\_FILE: name of file for initial  $\eta$ , e.g., ETA\_FILE= /Users/fengyanshi/work/input/CVV\_H.grd, data format is the same as depth data.

U\_FILE: name of file for initial  $u$ , e.g., U\_FILE= /Users/fengyanshi/work/input/CVV\_U.grd, data format is the same as depth data.

V\_FILE: name of file for initial  $v$ , e.g., V\_FILE= /Users/fengyanshi/work/input/CVV\_V.grd, data format is the same as depth data.

### **SPECIFICATION OF WAVEMAKER**

There is no wavemaker implemented in SHORECIRC.

### **SPECIFICATION OF PERIODIC BOUNDARY CONDITION**

( Note: only south-north periodic condition was implemented)

PERIODIC\_X: logical parameter for periodic boundary condition in x direction, T - periodic, F - wall boundary condition.

PERIODIC\_Y: logical parameter for periodic boundary condition in x direction.

Num.Transit: grid numbers needed to make periodic condition for SWAN. The reason to set this parameter is that SWAN doesn't have an option for periodic boundary condition. In this implementation, a periodic boundary condition is implemented by making a transition from a left array ( count to Num.Transit from left boundary) to a right array.

### **SPECIFICATION OF SPONGE LAYER**

SPONGE\_ON: logical parameter, T - sponge layer, F - no sponge layer.

Sponge\_west\_width: width (m) of sponge layer at west boundary.

Sponge\_east\_width: width (m) of sponge layer at east boundary.

Sponge\_south\_width: width (m) of sponge layer at south boundary.

Sponge\_north\_width: width (m) of sponge layer at north boundary

R\_sponge: decay rate in sponge layer. Its values are between 0.85 ~ 0.95.

A\_sponge: maximum damping magnitude. The value is ~ 5.0.

### **SPECIFICATION OF OBSTACLES**

OBSTACLE\_FILE: name of obstacle file. 1 - water point, 0 - permanent dry point. Data dimension is (Mglob × Nglob). Data format is the same as the depth data.

### **SPECIFICATION OF PHYSICS**

Cd: quadratic bottom friction coefficient

nu\_bkgd : background eddy viscosity parameter.

### **SPECIFICATION OF NUMERICS**

Time\_Scheme: stepping option, Runge\_Kutta or Predictor\_Corrector (not suggested for this version).

HIGH\_ORDER: spatial scheme option, FOURTH for the fourth-order, THIRD for the third-order, and SECOND for the second-order (not suggested for Boussinesq modeling).

CONSTRUCTION: construction method, HLL for HLL scheme, otherwise for averaging scheme.

CFL: CFL number, CFL ~ 0.5.

FroudeCap: cap for Froude number in velocity calculation for efficiency. The value could be 5 ~ 10.0.

MinDepth: minimum water depth (m) for wetting and drying scheme. Suggestion: MinDepth = 0.001 for lab scale and 0.01 for field scale.

MinDepthFrc: minimum water depth (m) to limit bottom friction value. Suggestion: MinDepthFrc = 0.01 for lab scale and 0.1 for field scale.

### **SPECIFICATION OF TIDAL RESIDUAL**

T\_INTV\_mean: time-averaging interval for Eulerian mean current and elevation. Note: use -DRESIDUAL in Makefile to make this option active.

## **SPECIFICATION OF SEDIMENT CALCULATION**

Note: set -DSEDIMENT in Makefile to make sediment module active

T\_INTV\_sed: time interval to call sediment module

Factor\_Morpho: morphology factor.

D\_50 :  $D_{50}$

D\_90 :  $D_{90}$

por: sediment porosity

RHO: water density

nu\_water: water eddy viscosity

S\_sed: specific gravity

SOULSBY: logical parameter for Soulsby (1997) total load formula, T = true, F = false

z0:  $z_0$ , bed roughness length.

KOBAYASHI: logical parameter for KOBAYASHI's formula, T = true, F = false

angle\_x\_beach: coordinate rotation angle defined in Figure 1.

eB:  $e_B$ , suspension efficiency for energy dissipation rate due to wave breaking

ef :  $e_f$ , suspension efficiency for energy dissipation rate due to bottom friction

a.k:  $a$ , empirical suspended load parameter.

b.k :  $b$ , empirical bedload parameter.

TanPhi:  $\tan \phi$ , where  $\phi$  is the angle of internal friction of the sediment.

Gm:  $G_m$  for slope function ( $G_m = 10$ ).

fr: friction coefficient in Kobayashi.

Si.c: a coefficient in calculating  $P_b$ .

## **SPECIFICATION OF OUTPUT VARIABLES**

NumberStations: number of station for output. If NumberStations > 0, need input i,j in STATION\_FILE

DEPTH\_OUT: logical parameter for output depth. T or F.

U: logical parameter for output  $u$ . T or F.

V: logical parameter for output  $v$ . T or F.

ETA: logical parameter for output  $\eta$ . T or F.

HS: logical parameter for output of significant wave height  $H_s$ . T or F.

WFC: logical parameter for output of wave force. T or F.

WDIR: logical parameter for output of peak wave direction. T or F.

WBV: logical parameter for output of wave orbital velocity. T or F.

MASK: logical parameter for output of wetting-drying MASK. T or F.

SourceX: logical parameter for output of source terms in  $x$  direction. T or F.

SourceY: logical parameter for output of source terms in  $y$  direction. T or F.

UV3D: logical parameter for output of 3D structure. T or F.

Qstk: logical parameter for output of Stokes mass flux. T or F.

DepDt: logical parameter for output of depth variation rate. T or F.

Qsed: logical parameter for output of sediment transport rate. T or F.

## 5.5 Output

The output files are saved in the result directory defined by `RESULT_FOLDER` in `INPUT`. For outputs in ASCII, a file name is a combination of variable name and an output series number such as `eta_0001`, `eta_0002`, .... The format and read/write algorithm are consistent with a depth file. Output for stations is a series of numbered files such as `sta_0001`, `sta_0002` ....

## 6 Examples

### 6.1 An idealized case

An idealized case is carried out to demonstrate a model run under several most useful conditions, including tide, wave, and river conditions. Figure 5 shows an idealized bathymetry which is constructed by a plane slope from a depth of 10 m to -1 m (dry points, 1m above the mean water level) and a channel with a depth of 2m located at the center of the beach. A wave spectrum is specified at the south boundary. A tidal boundary condition (M2) is applied to the south boundary. River flux is provided at the inlet. The vertical wall boundary condition is applied to the west and east boundaries.

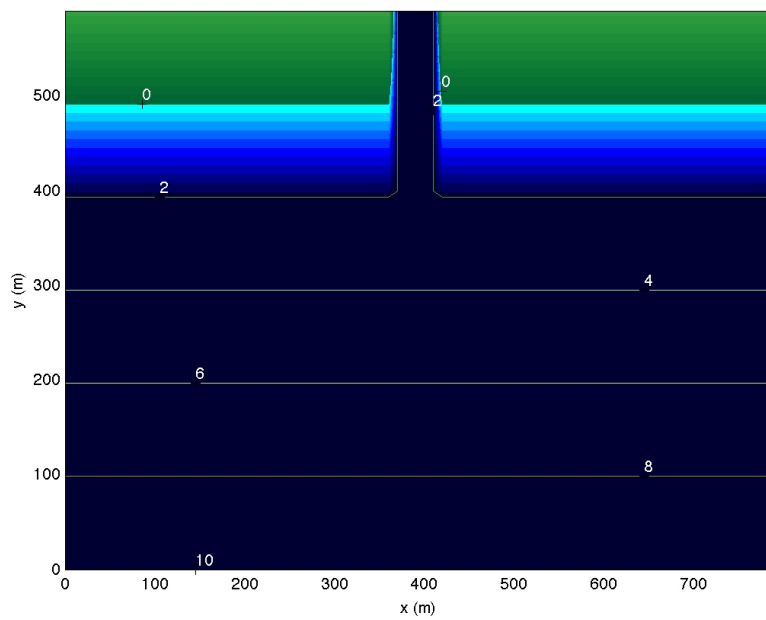


Figure 5: Idealized bathymetry.

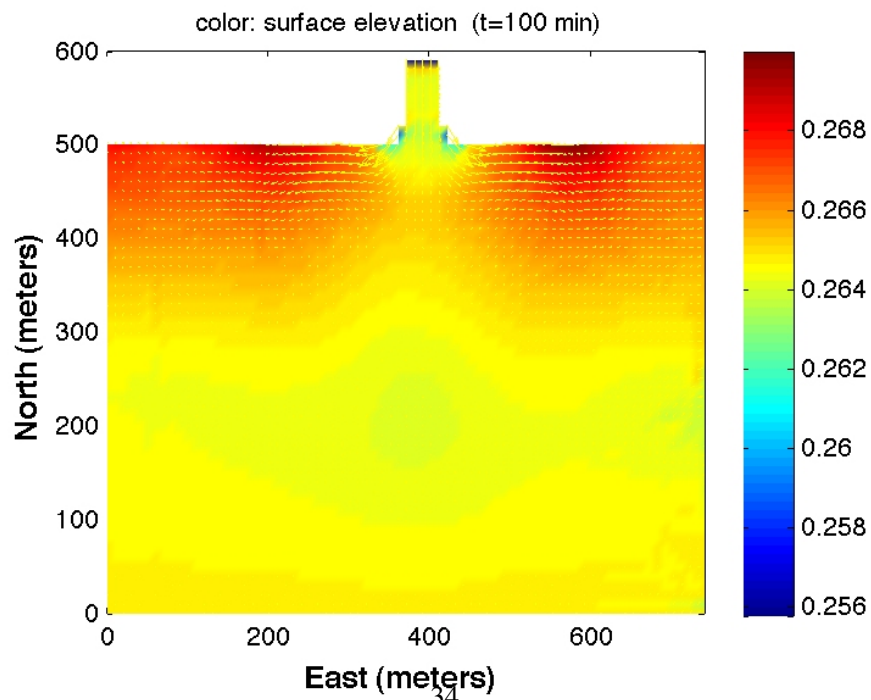
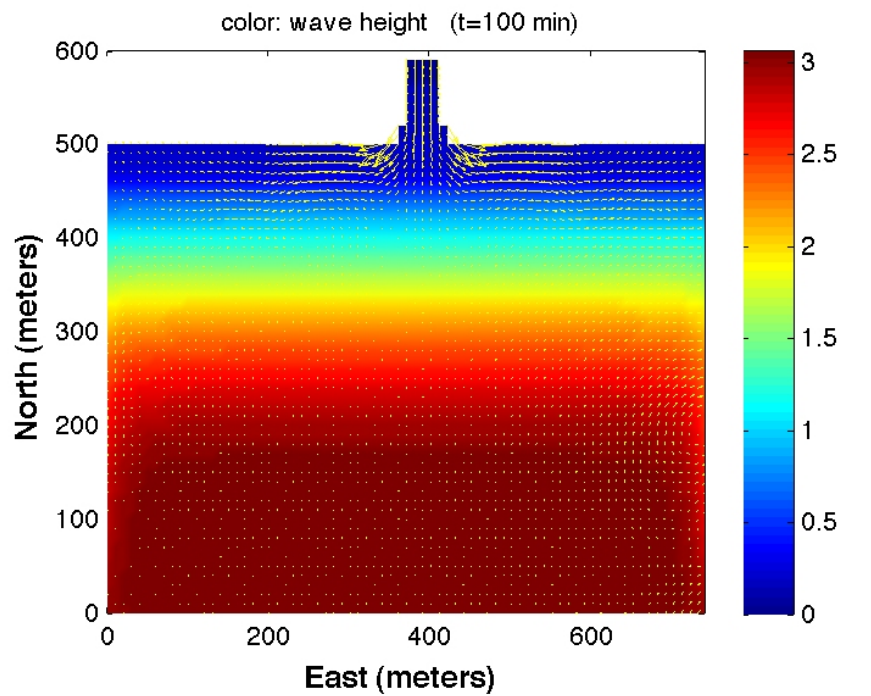


Figure 6: (Top panel) wave height (color) and currents. (Bottom panel) surface elevation (color) and currents.

The model grid is generated with  $dx=dy=10$  m and a dimension of 80 x 60. The grid generation file is provided in **/input/mkxyz\_inlet.f**. mkxyz produces **x\_inlet.txt**, **y\_inlet.txt**, and **dep\_inlet.txt** for SHORECIRC, and **xyyy\_swan\_inlet.txt** and **dep\_swan\_inlet.txt** for SWAN. Note that, in the test case, SWAN and SHORECIRC use the same grid, meaning the coordinates (x,y) for both models are the same. For a general application, the SWAN grid and SHORECIRC grid can be different.

The test needs a time series of waves for SWAN, tidal and river conditions for SHORECIRC. They are generated by programs: **mk\_wave\_field.m**, **mk\_tide.f90** and **mk\_river.f90**, respectively, provided in /input/. **mk\_wave\_field.m** generates time series of wave spectrum parameters saved in **wave\_field.txt**. **mk\_tide.f90** generates tidal constituents at every tidal boundary points, saved in **tide.txt**. **mk\_river.f90** makes a time series of river flux at river boundary points, saved in **river.txt**.

The specific model configurations are listed below.

### SWAN INPUT

```
SET 0 90 0.05 200 3 9.81 1025 0 0.10 CARTESIAN
MODE NONSTATIONARY TWODIMENSIONAL
CGRID CURV 79 59 EXC -99999.0 -99999.0 CIRCLE 36 0.038 0.5 43
READGRID COOR 1 './input/xyyy_swan_inlet.txt' 3
INPGRID BOTTOM CURV 0. 0. 79 59 EXC -99999.0
READINP BOTTOM 1 './input/dep_swan_inlet.txt' 3 0 FREE
WIND 0 150
BOUNDPAR1 SHAPESPEC JONSWP 3.3 PEAK DSPR DEGREES
BOUNDPAR2 SEGMENT IJ 0 0 79 0 CONSTANT FILE './input/wave_field.txt'
WCApping CSM
BREAKING CONSTANT 1.0 0.73
FRICTION JON
PROP BSBT
NUMERIC ACCUR .02 .02 .02 98 STAT 15 0.0
TEST 0,0
COMPUTE NONSTAT 20081114.160000 1 MI 20081114.230000
STOP
```

### WAVE CURRENT INTERATION

```
SWAN_RUN = T
SHORECIRC_RUN = T
```

WC\_BOUND\_WEST = 5  
WC\_BOUND\_EAST = 5  
WC\_BOUND\_SOUTH = 5  
WC\_BOUND\_NORTH = 0  
WC\_LAG = 1800.0

#### **PARALLEL INFO**

PX = 2  
PY = 2

#### **SHORECIRC INPUT**

DEPTH\_TYPE = DATA  
DEPTH\_FILE = **../input/dep\_inlet.txt**  
RESULT\_FOLDER = /Users/tmp/  
PLOT\_INTV = 120.0  
PLOT\_INTV\_STATION = 10.0  
SCREEN\_INTV = 120.0  
CORI\_CONSTANT = T  
LATITUDE = 34.1  
X\_FILE = **../input/x\_inlet.txt**  
Y\_FILE = **../input/y\_inlet.txt**  
ETA\_CLAMPED = T  
FLUX\_CLAMPED = T  
TIDE\_FILE = **../input/tide\_inlet.txt**  
FLUX\_FILE = **../input/river.txt**  
Cd = 0.0026  
Time\_Scheme = Runge\_Kutta  
HIGH\_ORDER = FOURTH  
CONSTRUCTION = HLLC  
CFL = 0.5  
FroudeCap = 0.8  
MinDepth=0.01  
MinDepthFrc = 0.01

NumberStations = 0

DEPTH\_OUT = T

U = T

V = T

ETA = T

HS = T

MASK = T

Figure 6 shows wave height (color) and currents (top panel) and surface elevation (color) and currents (bottom panel) at  $t = 100$  min. The figure was plotted using `plot_hs_uv.m` provided in `/postprocessing/`.

## 6.2 Simulation of longshore currents

Wave induced longshore current variation is first described by cross-shore momentum balance with known radiation stress associated with gravity waves (Longuet-Higgins 1970b). In a horizontal two dimensional beach, the nonlinear interaction terms between cross shore and longshore currents represent a dispersive mechanism that has an effect similar to turbulent mixing but an order of magnitude stronger (Svendsen et al. 1994). In NearCoM-TVD the alongshore current velocity can be represented as function of distance from the breaking line with a horizontal eddy viscosity. The results computed by NearCoM-TVD with a consideration of 2D horizontal mixing produce higher dissipation than that of Longuet-Higgins one dimensional theory Figure 7.

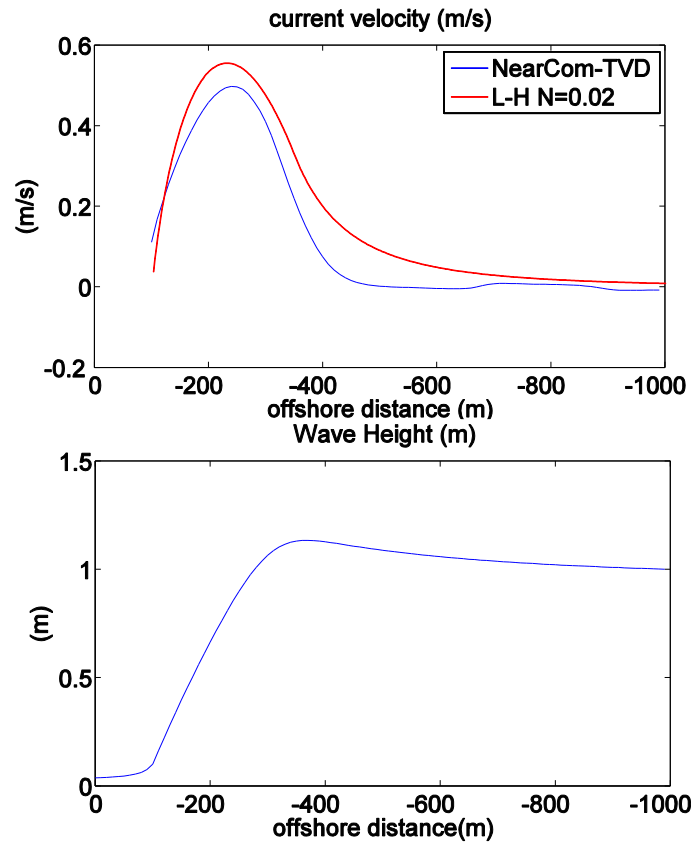


Figure 7: For the giving wave condition of wave height=1m, wave incident angle = 10 degree (a) Comparison of longshore current velocity profiles computed by NearCoM-TVD (blue) and Longuet-Higgins (1970b) (red). The breaker line location of Longuet-Higgins formula is given as  $X_B = -250$  m (b) Wave height distribution computed by NearCoM-TVD (SWAN).

Figure 8 shows an idealized bathymetry which is constructed by a plane slope (1/100) from a depth of 9 m to -1 m. A wave spectrum with incident angle 10 degree is specified at the south boundary. The vertical periodic boundary condition is applied to the west and east boundaries.

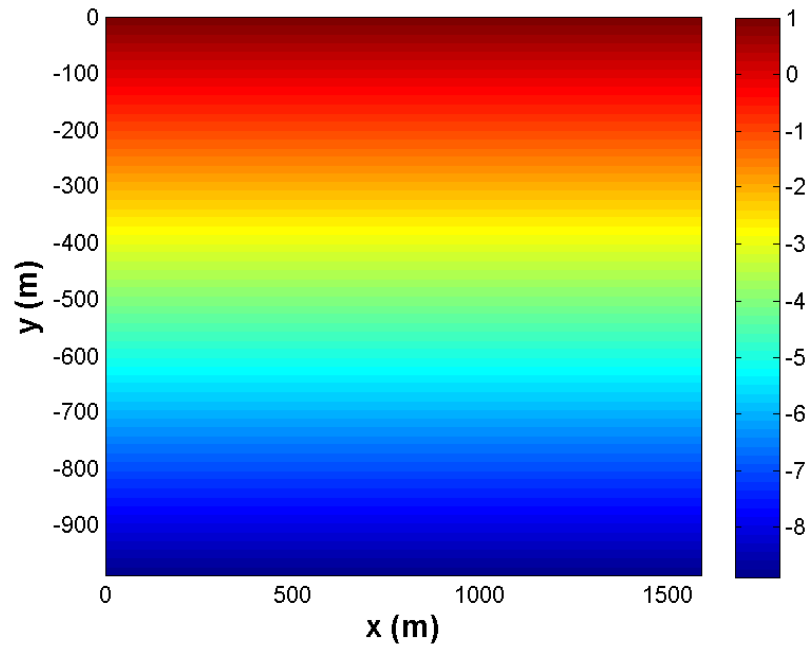


Figure 8: Idealized bathymetry.

The model grid is generated with  $dx=dy=10$  m with a constant slope. The grid generation file is provided in `/input/ mkxyz.f`. `mkxyz` produces `x.txt`, `y.txt`, and `dep.txt` for SHORECIRC, and `xyy_swan.txt` and `dep_swan.txt` for SWAN. The test only needs a time series of `wave_field.txt` generated by programs: `mk_wave_field.m`. To run this case, the `ETA_CLAMPED` and `FLUX_CLAMPED` in INPUT should be defined as F.

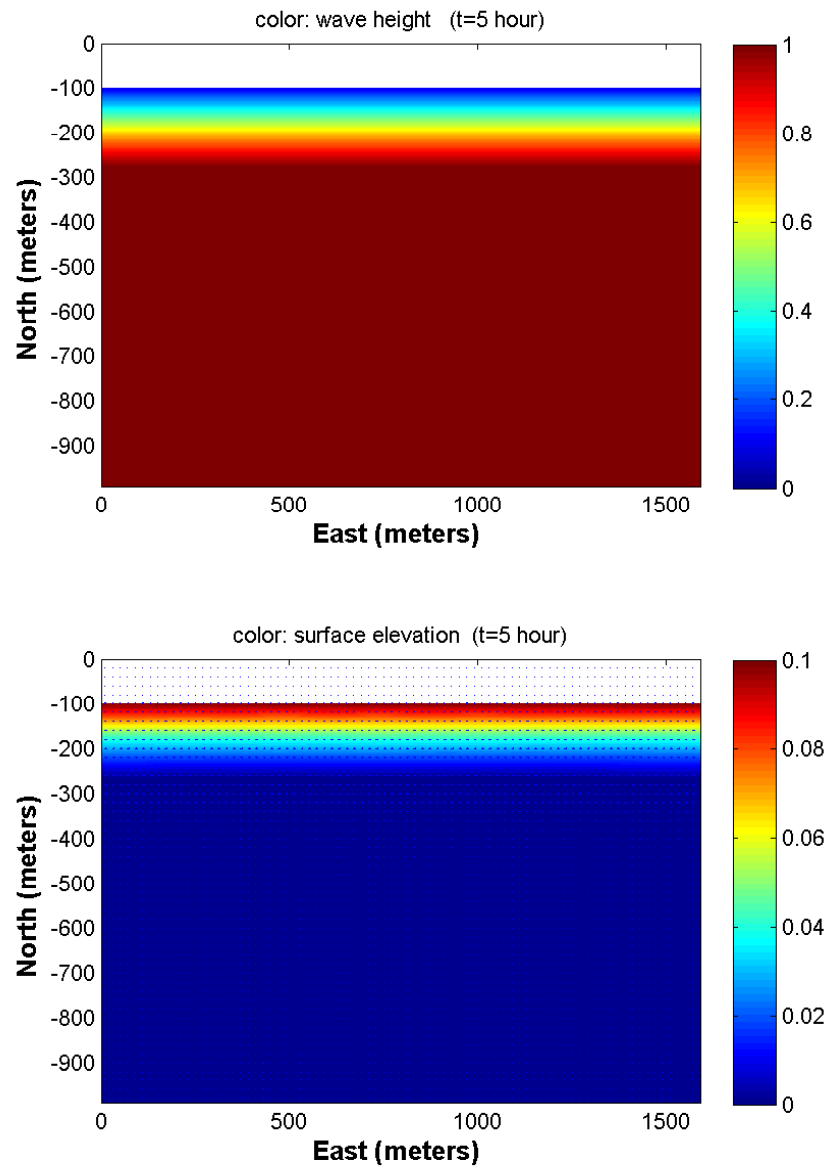


Figure 9: (Top panel) wave height (Bottom panel) current velocity

## 7 Appendix A: Extended form of tensor expression

Coordinate transformation is performed between  $x_\alpha$  or  $(x, y)$  and  $\xi^\alpha$  or  $(\xi^1, \xi^2)$ , where subscripts represent Cartesian and superscripts represent contravariant components in a generalized coordinate system. Some basic formulas or identities are used in the coordinate transformation and are listed below.

Relation between the Cartesian  $u_\alpha$  and the contravariant  $u^\alpha$ :

$$u^\alpha = u_\beta L_\beta^\alpha \quad (69)$$

where

$$L_\beta^\alpha = \frac{\partial \xi^\alpha}{\partial x_\beta} \quad (70)$$

Identity:

$$\frac{\partial}{\partial \xi^\alpha} (J L_\beta^\alpha) \equiv 0 \quad (71)$$

Relation between the Cartesian derivative and the contravariant derivative:

$$\frac{\partial F}{\partial x_\alpha} = L_\alpha^\beta \frac{\partial F}{\partial \xi^\beta} \quad (72)$$

Using the identity (71), (72) can be written in a different form as

$$\frac{\partial F}{\partial x_\alpha} = \frac{1}{J} \frac{\partial F J L_\alpha^\beta}{\partial \xi^\beta} \quad (73)$$

The pressure gradient term and other first-order tensor term can be easily transformed between the Cartesian and generalized curvilinear coordinates using (72) and (73). The radiation stresses and shear stresses contain more terms after coordinate transformation. The example of transformation for shear stress terms is demonstrated below.

$\tau_{\alpha\beta}$  in Cartesian coordinates can be expressed as

$$\tau_{\alpha\beta} = \mu_t \left( \frac{\partial u_\alpha}{\partial x_\beta} + \frac{\partial u_\beta}{\partial x_\alpha} \right) \quad (74)$$

After coordinate transformation,

$$\tau_{\alpha\beta} = \mu_t \left( L_\beta^\gamma \frac{\partial u_\alpha}{\partial \xi^\gamma} + L_\alpha^\gamma \frac{\partial u_\beta}{\partial \xi^\gamma} \right) \quad (75)$$

For coding, the extended form of (75) can be written as

$$\tau_{11} = 2\mu_t (L_1^1 u_{\xi^1} + L_1^2 u_{\xi^2}) \quad (76)$$

$$\tau_{12} = \tau_{21} = \mu_t (L_2^1 u_{\xi^1} + L_2^2 u_{\xi^2} + L_1^1 u_{\xi^1} + L_2^1 u_{\xi^2}) \quad (77)$$

$$\tau_{22} = 2\mu_t(L_2^1 u_{\xi_1} + L_2^2 u_{\xi_2}) \quad (78)$$

The shear stress terms can be written as

$$J \frac{\partial}{\partial x_\beta} (H \tau_{\alpha\beta}) = \frac{\partial}{\partial \xi^\gamma} (\tau_{\alpha\beta} J H L_\beta^\gamma) = J L_\beta^\gamma \frac{\partial}{\partial \xi^\gamma} (H \tau_{\alpha\beta}) \quad (79)$$

In the code,  $L_\beta^\alpha$  is defined as  $L_{\alpha\beta}$ . To keep a consistency with the code, we use  $L_{\alpha\beta}$  and  $\xi_\alpha$  to represent  $L_\beta^\alpha$  and  $\xi^\alpha$ , respectively, in the following extended expressions.

The shear stress terms in the  $x$ -direction can be expressed as

$$\begin{aligned} & J L_{11} (H \tau_{11})_{\xi_1} + J L_{21} (H \tau_{11})_{\xi_2} + J L_{12} (H \tau_{12})_{\xi_1} + J L_{22} (H \tau_{12})_{\xi_2} \\ &= J L_{11} \mu_t [2 H L_{11} u_{\xi_1 \xi_1} + 2 u_{\xi_1} (H L_{11})_{\xi_1} + 2 H L_{21} u_{\xi_1 \xi_2} + 2 u_{\xi_2} (H L_{21})_{\xi_1}] \\ &+ J L_{12} \mu_t [2 H L_{11} u_{\xi_1 \xi_2} + 2 u_{\xi_1} (H L_{11})_{\xi_2} + 2 H L_{21} u_{\xi_2 \xi_2} + 2 u_{\xi_2} (H L_{21})_{\xi_2}] \\ &+ J L_{12} \mu_t [H L_{12} u_{\xi_1 \xi_1} + u_{\xi_1} (H L_{12})_{\xi_1} + H L_{22} u_{\xi_1 \xi_2} + u_{\xi_2} (H L_{22})_{\xi_1} \\ &\quad + H L_{11} v_{\xi_1 \xi_1} + v_{\xi_1} (H L_{11})_{\xi_1} + H L_{12} v_{\xi_1 \xi_2} + v_{\xi_2} (H L_{12})_{\xi_1}] \\ &+ J L_{22} \mu_t [H L_{12} u_{\xi_1 \xi_2} + u_{\xi_1} (H L_{12})_{\xi_2} + H L_{22} u_{\xi_2 \xi_2} + u_{\xi_2} (H L_{22})_{\xi_2} \\ &\quad + H L_{11} v_{\xi_1 \xi_2} + v_{\xi_1} (H L_{11})_{\xi_2} + H L_{12} v_{\xi_2 \xi_2} + v_{\xi_2} (H L_{12})_{\xi_2}] \end{aligned} \quad (80)$$

and in the  $y$ -direction as,

$$\begin{aligned} & J L_{11} (H \tau_{21})_{\xi_1} + J L_{21} (H \tau_{21})_{\xi_2} + J L_{12} (H \tau_{22})_{\xi_1} + J L_{22} (H \tau_{22})_{\xi_2} \\ &= J L_{22} \mu_t [2 H L_{12} v_{\xi_1 \xi_2} + 2 v_{\xi_1} (H L_{12})_{\xi_2} + 2 H L_{22} v_{\xi_2 \xi_2} + 2 v_{\xi_2} (H L_{22})_{\xi_2}] \\ &+ J L_{12} \mu_t [2 H L_{12} v_{\xi_1 \xi_1} + 2 v_{\xi_1} (H L_{12})_{\xi_1} + 2 H L_{22} v_{\xi_1 \xi_2} + 2 v_{\xi_2} (H L_{22})_{\xi_1}] \\ &+ J L_{12} \mu_t [H L_{12} u_{\xi_1 \xi_2} + u_{\xi_1} (H L_{12})_{\xi_2} + H L_{22} u_{\xi_2 \xi_2} + u_{\xi_2} (H L_{22})_{\xi_2} \\ &\quad + H L_{11} v_{\xi_1 \xi_2} + v_{\xi_1} (H L_{11})_{\xi_2} + H L_{12} v_{\xi_2 \xi_2} + v_{\xi_2} (H L_{12})_{\xi_2}] \\ &+ J L_{11} \mu_t [H L_{12} u_{\xi_1 \xi_1} + u_{\xi_1} (H L_{12})_{\xi_1} + H L_{22} u_{\xi_1 \xi_2} + u_{\xi_2} (H L_{22})_{\xi_1} \\ &\quad + H L_{11} v_{\xi_1 \xi_1} + v_{\xi_1} (H L_{11})_{\xi_1} + H L_{12} v_{\xi_1 \xi_2} + v_{\xi_2} (H L_{12})_{\xi_1}] \end{aligned} \quad (81)$$

## 8 References

- Casulli, V. and Cheng, R. T., 1992, "Semi-implicit finite difference methods for three-dimensional shallow water flow", *Int. J. Numer. Method Fluid*, 15 (6), 629-648.
- Erduran, K. S., Ilic, S., and Kutija, V., 2005, "Hybrid finite-volume finite-difference scheme for the solution of Boussinesq equations", *Int. J. Numer. Meth. Fluid.*, 49, 1213-1232.
- Gottlieb, S., Shu C.-W., and Tadmire, E., 2001, "Strong stability-preserving high-order time discretization methods", *SIAM Review*, 43 (1), 89 - 112.
- Haas, K. A., I. A. Svendsen, M. C. Haller, and Q. Zhao, 2003, Quasi-three-dimensional modeling of rip current systems, *J. Geophys. Res.*, 108, C7, 3216, doi:10.1029/2001JC001313.

- Kim D. H., Cho, Y. S., and Kim, H. J., 2008, "Well-balanced scheme between flux and source terms for computation of shallow-water equations over irregular bathymetry", *Journal of Engineering Mechanics*, 134, 277-290.
- Kim, D. H., Lynett, P. J. and Socolofsky, S. A., 2009, "A depth-integrated model for weakly dispersive, turbulent, and rotational fluid flows", *Ocean Modeling*, 27, 198-214.
- Kim, D. H., 2009, "Turbulent flow and transport modeling by long waves and currents", Ph.D. dissertation, Texas A& M University.
- Kirby, J. T., Wei, G., Chen, Q., Kennedy, A. B. and Dalrymple, R. A., 1998, "FUNWAVE 1.0, Fully nonlinear Boussinesq wave model. Documentation and users manual". Report CACR-98-06, Center for Applied Coastal Research, Department of Civil and Environmental Engineering, University of Delaware.
- Kirby, J. T. and Dalrymple, R. A., 1992, "Combined Refraction/Diffraction Model REF/DIF 1, Version 2.4. Documentation and User's Manual", Research Report No. CACR-92-04, Center for Applied Coastal Research, Department of Civil Engineering, University of Delaware, Newark.
- Kirby, J. T., Shi, F., Harris, J. C., and Grilli, S. T., 2011, "Sensitivity analysis of trans-oceanic tsunami propagation to dispersive and Coriolis effects", in preparation.
- Lynett, P. J., Wu, T.-R. and Liu, P. L.-F., 2002, "Modeling wave runup with depth-integrated equations", *Coastal Engineering*, 46, 89-107.
- Naik, N. H., Naik, V. K., and Nicoules, M., 1993, "Parallelization of a class of implicit finite difference schemes in computational fluid dynamics", *International Journal of High Speed Computing*, 5: 1-50.
- Newberger, P. A. and Allen, J. S., 2007, Forcing a three-dimensional, hydrostatic, primitive-equation model for application in the surf zone: 1. Formulation, *J. Geophys. Res.*, 112, C08018, doi: 10.1029/2006JC003472
- Ning, D. Z., Zang, J., Liang, Q., Taylor, P. H., and Borthwick, A. G. L., 2008, "Boussinesq cut-cell model for non-linear wave interaction with coastal structures", *International Journal for Numerical Methods in Fluids*, 57 (10), 1459-1483.
- Putrevu, U. and I. A. Svendsen, 1999, Three-dimensional dispersion of momentum in wave-induced nearshore currents, *Eur. J. Mech. B/Fluids*, 83-101.
- Roeber, V., Cheung, K. F., and Kobayashi, M. H., 2010, "Shock-capturing Boussinesq-type model for nearshore wave processes", *Coastal Engineering*, 57, 407-423.

- Rogers, B. D., Borthwick, A. G. L., and Taylor, P. H., 2003, "Mathematical balancing of flux gradient and source terms prior to using Roe's approximate Riemann solver", *Journal of Computational Physics*, 192, 422-451.
- Shi, F., Kirby, J. T., Newberger, P. and Haas, K., 2005, "NearCoM masetr program for nearshore community model, Version 2005.4 - Documentation and user's manual", Research Report No. CACR-05-10, Center for Applied Coastal Research, Dept. of Civil and Environmental Engineering, Univ. of Delaware, Newark.
- Shi, F., Kirby, J. T., Tehranirad, B. and Harris, J. C., 2011a, FUNWAVE-TVD, users' manual and benchmark tests, Center for Applied Coastal Research Report, CACR 2011-04, University of Delaware, Newark, Delaware.
- Shi, F., Kirby, J. T., Harris, J. C., Geiman, J. D., and Grilli, S. T., 2011b, "A high-order adaptive time-stepping TVD solver for Boussinesq modeling of breaking waves and coastal inundation", *Ocean Modelling*, doi:10.1016/j.ocemod.2011.12.004.
- Shi, F., Sun, W. and Wei, G., 1998, A WDM method on generalized curvilinear grid for calculation of storm surge flooding, *Applied Ocean Research*, 19(4), 275-282.
- Shi, F. and Sun, W., 1995, A variable boundary model of storm surge flooding in generalized curvilinear grids, *International Journal for Numerical Methods in Fluids*, 21 (8), 642-651.
- Shi, F., Svendsen, I. A., Kirby, J. T., and Smith, J. M., 2003, A curvilinear version of a Quasi-3D nearshore circulation model, *Coastal Engineering*, 49 (1-2), 99-124
- Shiach, J. B. and Mingham, C. G., 2009, "A temporally second-order accurate Godunov-type scheme for solving the extended Boussinesq equations", *Coastal Engineering*, 56, 32-45.
- Sitanggang, K. I. and Lynett, P., 2005, "Parallel computation of a highly nonlinear Boussinesq equation model through domain decomposition", *Int. J. Num. Meth. Fluids*, **49**, 57-74.
- Smagorinsky, J., 1963, "General circulation experiments with the primitive equations. I. The basic experiment", *Mon. Weather Rev*, 91, 99-165.
- Svendsen I. A., K. A. Haas, and Q. Zhao, 2004, Quasi-3D Nearshore Circulation Model SHORE-CIRC: Version 2.0, Research Report, Center for Applied Coastal Research, University of Delaware.
- Tehranirad, B., Shi, F., Kirby, J. T., Harris, J. C. and Grilli, S., 2011, "Tsunami benchmark results for fully nonlinear Boussinesq wave model FUNWAVE-TVD, Version 1.0", Research Report No. CACR-11-02, Center for Applied Coastal Research, University of Delaware.
- Tonelli, M. and Petti, M., 2009, "Hybrid finite volume - finite difference scheme for 2DH improved Boussinesq equations", *Coast. Engrng.*, **56**, 609-620.

- Tonelli, M. and Petti, M., 2010, "Finite volume scheme for the solution of 2D extended Boussinesq equations in the surf zone", *Ocean Engrng.*, **37**, 567-582.
- Toro, E. F., 2009, *Riemann solvers and numerical methods for fluid dynamics: a practical introduction*, Third edition, Springer, New York.
- Yamamoto, S., Daiguji, H., 1993, "Higher-order-accurate upwind schemes for solving the compressible Euler and NavierStokes equations", *Computers and Fluids*, 22 (2/3), 259270.
- Yamamoto, S., Kano, S. and Daiguji, H, 1998, "An efficient CFD approach for simulating unsteady hypersonic shockshock interference flows", *Computers and Fluids* 27 (56), pp. 571-580.
- Zhou, J. G., Causon, D. M., Mingham C. G., and Ingram, D. M., 2001, "The surface gradient method for the treatment of source terms in the shallow-water equations", *Journal of Computational Physics*, 168, 1-25.